JCTC Journal of Chemical Theory and Computation

Effect of Force Field Parameters on Sodium and Potassium Ion Binding to Dipalmitoyl Phosphatidylcholine Bilayers

Arnau Cordomí,[†] Olle Edholm,[‡] and Juan J. Perez*,[†]

Department d'Enginyeria Química, Technical University of Catalonia (UPC), Avenue Diagonal 647, 08028 Barcelona, Spain, and, Theoretical Biological Physics, Royal Institute of Technology (KTH), SE-10691 Stockholm, Sweden

Received February 12, 2009

Abstract: The behavior of electrolytes in molecular dynamics simulations of zwitterionic phospholipid bilayers is very sensitive to the force field parameters used. Here, several 200 ns molecular dynamics of simulations of dipalmitoyl phosphotidylcholine (PC) bilayers in 0.2 M sodium or potassium chloride using various common force field parameters for the cations are presented. All employed parameter sets give a larger number of Na^+ ions than K^+ ions that bind to the lipid heads, but depending on the parameter choice quite different results are seen. A wide range of coordination numbers for the Na^+ and K^+ ions is also observed. These findings have been analyzed and compared to published experimental data. Some simulations produce aggregates of potassium chloride, indicating (in accordance with published simulations) that these force fields do not reproduce the delicate balance between salt and solvated ions. The differences between the force fields can be characterized by one single parameter, the electrostatic radius of the ion, which is correlated to σ_{MO} (M represents Na^+/K^+), the Lennard-Jones radius. When this parameter exceeds a certain threshold, binding to the lipid heads is no longer observed. One would, however, need more accurate experimental data to judge or rank the different force fields precisely. Still, reasons for the poor performance of some of the parameter sets are clearly demonstrated, and a quality control procedure is provided.

Introduction

Biological membranes are essential for cell integrity, providing a physical barrier between the interior and exterior of a cell, as well as a separation between different inner compartments. In addition, membranes provide a matrix to hold many types of proteins involved in important cell functions and, consequently, play a key role for regulation of biological processes. At physiological conditions, the membranes are in contact with an aqueous solution that contains ions like Na^+, K^+, Ca^{2+}, Mg^{2+}, and Cl^- and, therefore, the study of interactions between lipids, water molecules, and ions is of great importance.[1] Experiments from the last decade show that ions play an essential role not only in modulating the structure, dynamics, and stability of membranes, but also in the binding and insertion of proteins, membrane fusion, and transport across them.[2] Current knowledge of the interplay between ions and biological membranes is still scarce due to experimental difficulties. However, spectroscopic experiments reveal that cations bind to negatively charged moieties in the lipid head groups of charged[3−7] or zwitterionic phosphatidylcholine (PC) lipids,[8−15] whereas anions, like chloride, remain solvated outside the bilayer. Moreover, images of averaged positions of ions in gel-phase PC bilayers have recently been resolved using atomic force microscopy, revealing that the negatively charged phosphate groups share the charge distributions generated by mobile cations.[16]

Despite early experimental evidence that ions may alter the structural properties of lipid bilayers,[17,18] the difficulties associated with the precise characterization of these still leave

* Corresponding author. Phone: +34934016679. Fax: +34934017150. E-mail: juan.jesus.perez@upc.edu.

[†] Technical University of Catalonia.

[‡] Royal Institute of Technology.

10.1021/ct9000763 CCC: $40.75
Published on Web 07/06/2009

several issues to be uncovered, especially for zwitterionic bilayers. Thus, it is well established that bound ions alter the orientation of lipid head groups,[19−23] and there is also growing evidence that they affect the order of the lipid chains, leading to bilayer thickening. Effects on the gel to liquid crystalline phase transition of phosphatidylcholine (PC) bilayers in contact with certain mono- and divalent ions have also been reported.[24,25] Additionally, effects on heat capacity[26] and nanomechanical properties of zwitterionic PC lipids[27] suggest that the binding of ions reduces the area per lipid. This has recently been observed in X-ray studies[28] of PC bilayers in solution containing Na^+ or Ca^{2+} ions at >1 M concentrations, while an effect was not observed with K^+ ions in the same concentration range.[29]

Atomistic molecular dynamics (MD) simulations of lipid bilayers have emerged in the last years as a useful technique capable of providing a detailed microscopic picture of the interactions and processes occurring in biological membranes which are not always accessible experimentally. The complexity of real membranes containing different proteins, lipids, and other molecules makes atomic scale modeling of such systems computationally unaffordable. The study of one-component model lipid bilayers, however, presently is feasible and has been the focus of a large number of reports published in the last few years, being pivotal in providing new insights into these matters.[30−36] MD simulations of lipid bilayers in contact with electrolytes support that cations bind to the head groups of zwitterionic lipids.[5,6,26,37−43] It has, however, been observed that the equilibrium properties of such systems are sensitive to the force field parameters used for phospholipids,[44] water molecules,[45−48] and ions[49] used in the simulations. The ion parameters are the most critical ones due to the fragmentary experimental knowledge of the structural properties of ionic solutions at finite concentration. A recent systematic comparison using different widely used parameters in simulations of an aqueous solution of sodium chloride showed that, even if all the parameters could describe the physical properties governed by the ion hydration shell in its immediate neighborhood, ion−ion radial distribution functions exhibited substantial differences.[49] In the same direction, an unbalance in the parameters of some alkali cations has recently been reported to be the origin of serious potassium chloride aggregation problems that could affect the quality of the generated MD trajectories.[50−53]

Recent MD simulations of PC lipid bilayers published in the literature reveal large differences in the degree of K^+ ion binding to lipid oxygens − from negligible to substantial − depending on the parameters used for K^+ and Cl^- ions and, therefore, on the structural electrostatic properties of the associated bilayer.[41,43,54−56] This indicates that it is an important task to further investigate the effect of ion parameters on lipid bilayer simulations in order to improve the understanding of the different binding behavior reported for K^+ compared to that of Na^+ and Ca^{2+}.[28,29] The present work aims at rationalizing the effect of monovalent ion parameters on the degree of binding of such ions to PC bilayers using atomistic MD simulations. For this purpose, a set of seventeen simulations of dipalmitoyl phosphatidylcholine (DPPC) bilayers (Figure 1) in contact with 0.2 M aqueous solutions of sodium or potassium chloride were carried out using an ample variety of parameters available in the literature for Na^+ and K^+. The present study provides a perspective on the performance of the different parameters and, furthermore, provides a guide for the selection, or further optimization, of ion parameters. Finally, it is concluded that the number of bound alkali ions per lipid drops linearly with the Lennard-Jones (LJ) parameter, σ.[57] This affects also other properties, such as the area per lipid and the head group dipole tilt angle.

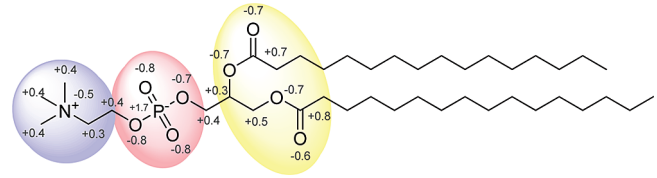

Figure 1. Chemical structure of a DPPC lipid with the partial charges given according to the Berger force field[31] (see Methods Section). Colors indicate the following regions: choline (blue), phosphate (red), and carbonyls (yellow).

Methods

Simulation Setup. All computer simulations were performed with the GROMACS 3.3.2 package[58,59] using the same protocols described elsewhere.[41] DPPC lipids were modeled using a slight modification of the parameters developed by Berger and collaborators.[31] Parameters for alkali ions selected for the present work are listed in Table I and were retrieved from different sources. They will be referred to as: Jorgensen,[60] GROMOS,[61] CHARMM,[62] Dang,[63] Jensen,[64] AMBER, and OPLS (both derived from the original Åqvist parameters[65]) throughout the manuscript respectively. The implementation of the OPLS-AA[66] force field in GROMACS was used for the Jorgensen and OPLS parameters. All the simulations employed Åqvist[65] parameters for Cl^- ions and the TIP3P model for water molecules.[67]

As starting configurations, a previous 40 ns simulation of a DPPC bilayer with water and sodium chloride[41] was used. This system consists of 256 lipids, ∼17 000 water molecules, corresponding to a hydration of 66 waters per lipid, and 61 Na^+ and 61 Cl^- ions, giving a concentration of sodium chloride of about 0.2 M. The initial size of the periodic simulation boxes was 8.1 × 8.1 × 12.7 nm^3 (*XYZ*), which corresponds to an area per lipid of about 0.58 nm^2. The thickness of the water layer is about 8 nm, which gives a fully hydrated system by wide margins.[43] Systems containing KCl were generated by replacing the sodium ions in the starting box for the NaCl systems. Each simulation was run for 200 ns of which the first 100 ns were considered as equilibration and, consequently, all averages were calculated only over the last 100 ns, since it is well-known that equilibration times for this kind of system are long.[40] Figure 2 shows an equilibrated DPPC/NaCl system after 200 ns of simulations.

Details about the Ion−Lipid Potential. In a classical force field, the ion−water/lipid oxygen potential energy function consists of two terms: one electrostatic, V_{MO}^{Coul}, and

Table I. LJ Parameters for Na^+ and K^+ Ions Compared in the Present Study and Phosphate Lipid Oxygen Parameters

	parameter set	σ (nm)	ε (kJ/mol)	B[g]	A[g]
Na^+	Jorgensen[a]	0.190	6.7288	1.256×10^{-3}	5.862×10^{-8}
	CHARMM[b]	0.224	0.1963	9.998×10^{-5}	1.273×10^{-8}
	Dang[c]	0.235	0.5439	3.664×10^{-4}	6.172×10^{-8}
	GROMOS[d]	0.258	0.0618	7.207×10^{-5}	2.102×10^{-8}
	OPLS[e]	0.333	0.0116	6.335×10^{-5}	8.645×10^{-8}
	Jensen[f]	0.407	0.0021	3.804×10^{-5}	1.729×10^{-7}
K^+	CHARMM[b]	0.314	0.3640	1.402×10^{-3}	1.351×10^{-6}
	AMBER[e]	0.474	0.0014	6.194×10^{-5}	6.990×10^{-7}
	OPLS[e]	0.493	0.0014	7.931×10^{-5}	1.145×10^{-6}
	Jensen[f]	0.517	0.0021	1.598×10^{-4}	3.051×10^{-6}
	GROMOS[d]	0.645	0.0001	1.638×10^{-5}	1.184×10^{-6}
O	Berger	0.296	0.8780	2.362×10^{-3}	1.589×10^{-6}

[a] Ref 60. [b] Ref 62. [c] Ref 63. [d] Ref 61. [e] Ref 65. [f] Ref 64. The different values for OPLS and AMBER respond to truncation on the conversions associated to each implementation. [g] B and A are given in kJ/mol·nm^6 and kJ/mol·nm^{12}.

one LJ, V_{MO}^{LJ}, with M being either Na^+ or K^+ and O standing for oxygen:

$$V_{MO}(r) = V(r)_{MO}^{Coul} + V(r)_{MO}^{LJ}$$

Both energies are functions of the distance, r, between the atoms. There are two equivalent, widely used ways to write the LJ potential, which both will be used here:

$$V_{MO}^{LJ}(r) = 4\varepsilon_{MO}\left[\left(\frac{\sigma_{MO}}{r}\right)^{12} - \left(\frac{\sigma_{MO}}{r}\right)^{6}\right] = \frac{A_{MO}}{r^{12}} - \frac{B_{MO}}{r^{6}}$$

In the first form, ε is the depth of the potential well, and σ is the distance at which the potential is zero, while the constants A and B, in the second expression, account for the strength of the repulsive part and the attractive parts separately. These MO parameters are obtained by averaging single atom ones, which originally have been obtained by a fit to reproduce experimental data.[68] Most force fields use a geometric mean for the ε parameters, but either a geometric or an arithmetic (also named Lorentz−Bertholet) mean may be used for the σ parameters. The geometric and arithmetic averages are similar unless parameters of the individual atoms are much different. Here simulations with both combination schemes have been performed when the different ways of averaging the σ's have produced differences that are larger than 0.003 nm.

One of the simplest ways to model free energies of solvation of cations in water is the Born approximation:

$$\Delta G_{born} = -\frac{1}{8\pi\varepsilon_o}\left(1 - \frac{1}{\varepsilon}\right)\frac{q^2e^2}{r_{eff}}$$

This depends only on the permittivity of the medium (ε), the charge of the cation, and the size of the cavity that it occupies (r_{eff}). The latter value is generally larger than the ionic radii (r_{ion}), since, otherwise, the expression would overestimate the energy. However, it is possible to estimate r_{eff} from the first peak in the radial distribution function (rdf) for M-water O pairs (r_{rdf})[25,69] as

$$r_{eff} = \frac{(2r_{rdf} - r_o)}{2}$$

where, r_o is the radius of the oxygen atom in a water molecule, which is approximately 0.14 nm.

Results and Discussion

Ion Binding and Coordination. For each simulation, the average number of alkali ions bound to the DPPC bilayer was determined. It was defined as the total number of ions located closer to at least one of the lipid oxygens smaller than the distance corresponding to the first peak in the M-lipid oxygen rdf. This means within 0.31 and 0.36 nm for Na^+ and K^+, respectively.[41] These numbers are listed as ions/lipid in Table II. Table II shows that, within every parameter set, the number of bound Na^+ ions is always larger than that of K^+. Moreover, between 0.09 and 0.24 Na^+ ions bind per lipid, which is between 37 to 99% of the total number of ions. Earlier studies,[41] in which higher ion concentrations also were used, indicate that sodium ions saturate the bilayer at about 0.3 Na^+ per lipid. K^+ ions bind to a lower extent, ranging between 0.00 and 0.14 ions per lipid, corresponding to 0 to 58% of the total number of ions. These results show that the degree of Na^+ and K^+ binding is extremely sensitive to force field parameters.

The ion coordination features reveal different characteristics of the binding in the simulations. In Table III, results from simulations with substantial ion binding (>0.03 ions per lipid) are listed. The coordination number (CN) of the ions, as determined from the M-water oxygen rdf's, varies between 5 and 6 for Na^+ and between 6 and 7 for K^+ with the phosphate and carbonyl oxygens of the lipids, water oxygens, and chloride as coordinating atoms. These numbers are in reasonable agreement with experiments as well as other computational predictions.[70] The preferred number of lipid oxygens in the first coordination shell is 4 or 5 for Na^+, whereas for K^+ the value range is between 2 and 5. The number of different lipids coordinating each Na^+ is mostly 2 or 3, while this number is between 1 and 3 for K^+. The average number of lipids per Na^+ ion is 2.4−2.9, in good agreement with the values of 2.85 and 3.1 reported by Gurtovenko[39] and Baker,[43] despite the differences in setup and system size. We also investigated the ionic preference between the carbonyl oxygens of the glycerol backbone and phosphate oxygens with different ion parameters. All simula-

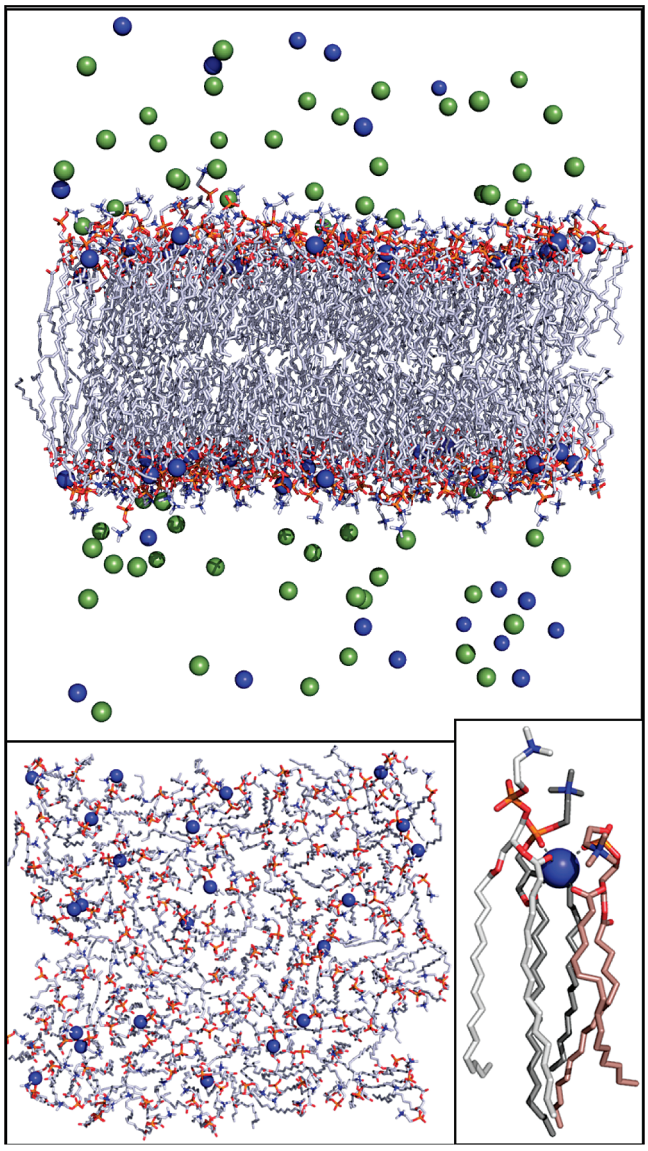

Figure 2. Snapshot of an equilibrated DPPC/NaCl system after 200 ns of MD simulations: (top) lateral view showing the bilayer and the location of Na^+ (blue) and Cl^- ions (green); (bottom-left) top view of a single layer showing the bound cations; and (bottom-right) details of a representative Na^+−DPPC complex with three lipids coordinating the ion to carbonyl and phosphate oxygens. The atoms are colored according to types, with lipid atoms represented as sticks and ions as spheres. The water molecules are not shown for better clarity.

tions suggest that both are important attractors for the ions, but that the phosphate oxygens are preferred, with average CN's of 1.9−2.7 and 1.4−2.2, for Na^+ and K^+, respectively, while the coordination numbers are smaller, 1.2−1.9 and 0.9−1.4, for the carbonyl oxygens (see Table III). The preference for one oxygen type or the other is not well-known experimentally,[16,25] and it seems to be strongly dependent on the force field employed for lipids, the water model, the system size and sampling. However, the values above are useful when comparing the performance of the different cation parameters.[38,43] It is interesting to note that both the average number of lipid oxygens coordinated to alkali ions and the number of lipids per ion bound exhibit a parallel trend (see Table III), which correlates with the extent of ion binding shown in Table II. This suggests, as will be shown later, that differences in these features between simulations may have the same origin. They may be correlated with the strength of the cation/oxygen interaction within each parameter set, which in turn is determined by the LJ radius.

Potassium Chloride Aggregation. Before describing the structural effects associated with the ionic binding to the lipid bilayer in the next section (Structural Effects), we want to stress that some of the K^+ parameters produce important artifacts in the simulations. Visual inspection of the final coordinates (after 200 ns) of each trajectory reveals in some cases the existence of large clusters of potassium chloride (containing essentially all ions in the system) arranged in a face-centered cubic lattice typical of alkali−chloride crystals.[71] Since a salt concentration of 0.2 M is much lower than the saturation limit, 3.2 M,[72] these aggregates should be considered as an artifact of the force field used in those simulations. This has already been observed in pure water/salt[50,52,53,73] and water/salt/DNA[50−52,74,75] systems. In the present work, these aggregation problems are found in the simulations using GROMOS[61] and Åqvist (AMBER and OPLS) potassium parameters[68] with the Lorentz−Bertholet combination rule. This agrees with a very recent study reporting artifacts found when using the Åqvist parameters, employing the same combination rule.[50] The LJ parameters for K^+ seem to be the main reason for this artifact, since test simulations using I^- or different Cl^- parameters did not change these results (data not shown). Second, similar aggregation problems have been reported for other water models.[50] Thus, it appears as if ε_{MM} values of 0.0014 kJ/mol or smaller combined with large σ_{MO} parameters leads to aggregation when the Lorentz−Bertholet combination rule is used. In contrast, the use of the geometric combination rule does not result in such artifacts. By the time this manuscript was being prepared, a corrected set of ion parameters to be used with the AMBER force field was reported in order to overcome this problem.[53] Interestingly, these new parameters for ion K^+ have a much smaller σ and a larger ε. The use of Åqvist parameters in conjunction with geometric averaging for the σ's in the AMBER force field has been proposed as an alternative fix.

K^+−Cl^- aggregation can be monitored through the K^+−Cl^- rdf at different time windows. Aggregation produces an increased second peak in the rdf at about 0.30 nm, due to transient contacts between ionic pairs, and the appearance of well-defined additional peaks at larger distances mainly at 0.55 and 0.70 nm (data not shown). The aggregation rate is slow at MD time scales, although it depends on the concentration. In the simulations presented here, typically 25−100 ns or more are required to obtain large clusters. Therefore, these artifacts were not detected until recently when such time scales became easily accessible in simulations, despite that most of the currently used ion parameters have been used for almost 20 years.[60,68] The process is faster if the initial positions of the K^+ ions are generated in the solvent instead of starting from sodium positions, where some are deep inside the lipid head group region (see Methods Section). A reanalysis of our previously reported 40 ns

Table II. Summary of Simulations and Results[a]

cation	source	comb. rule	σ_{MO} (nm)	A_{MO}[i]	area (nm^2)	dipole angle (°)	# ions per lipid	MCl aggregates	r_{eff}[j] (nm)	ΔG_{hyd}[k] (kJ/mol)
none	–	geom.	–	–	0.620	13	–	–	–	–
Na^+	Jorgensen[b]	geom.	0.237	3.05×10^{-7}	0.531	26	0.24	No	0.158	−434
	CHARMM[c]	geom.	0.260	1.60×10^{-7}	0.538	27	0.23	No	0.146	−470
	Dang[d]	geom.	0.266	3.47×10^{-7}	0.541	27	0.22	No	0.158	−434
	GROMOS[e]	geom.	0.276	1.82×10^{-7}	0.541	26	0.22	No	0.148	−463
	OPLS[f]	geom.	0.314	3.71×10^{-7}	0.562	22	0.16	No	0.166	−413
		arit.	0.315	3.78×10^{-7}	0.570	22	0.15	No	0.166	−413
	Jensen[g]	geom.	0.347	5.22×10^{-7}	0.576	19	0.11	No	0.176	−390
		arit.	0.352	6.10×10^{-7}	0.593	18	0.09	No	0.181	−380
K^+	CHARMM[c]	geom.	0.305	1.47×10^{-6}	0.579	21	0.14	No	0.198	−346
	GROMOS[e]	geom.	0.437	1.37×10^{-6}	0.602	15	0.04	No	0.202	−340
		arit.	0.471	3.34×10^{-6}	0.617	13	0.00	Yes	0.226	−303
	OPLS[f]	geom.	0.382	1.35×10^{-6}	0.600	16	0.04	no	0.202	−340
		arit.	0.395	1.99×10^{-6}	0.618	13	0.00	yes	0.215	−320
	AMBER[f]	geom.	0.374	1.04×10^{-6}	0.594	13	0.06	no	0.194	−353
		arit.	0.385	1.47×10^{-6}	0.619	13	0.00	yes	0.206	−333
	Jensen[g]	geom.	0.391	2.19×10^{-6}	0.603	14	0.03	no	0.214	−320
		arit.	0.407	3.49×10^{-6}	0.615	13	0.01	no	0.226	−303

[a] The combination rule accounts for how σ pairs are computed as a geometric or an arithmetic average. The standard deviations are in area per lipid 0.005 −0.008 nm^2, in number of bound ions per lipid less than 0.01, while the PN dipole angle has a broad distribution with a width of about 35°. [b] Ref 60. [c] Ref 62. [d] Ref 63. [e] Ref 61. [f] Ref 65. [g] Ref 64. [h] A in kJ/mol. [i] nm^{12}. [j] $r_{eff} = (2r_{rdf} - r_o)/2$. [k] ΔG_{hyd} from the Born approximation (see Methods Section).

Table III. Average Number of Lipid Oxygens of Different Types and Average Number of Lipids Coordinated to Each Bound Na^+ and K^+ ion Together with Standard Deviations

cation		comb. rule	no. of phosphate oxygens	no. of carbonyl oxygens	total no. of lipid oxygens	no. of lipids
Na^+	Jorgensen[a]	geom.	1.82 ± 0.07	2.65 ± 0.08	5.36 ± 0.08	2.92 ± 0.05
	CHARMM[b]	geom.	1.87 ± 0.07	2.30 ± 0.08	4.41 ± 0.08	2.78 ± 0.06
	Dang[c]	geom.	1.82 ± 0.07	2.47 ± 0.12	4.62 ± 0.12	2.82 ± 0.07
	GROMOS[d]	geom.	1.78 ± 0.07	2.31 ± 0.10	4.27 ± 0.13	2.70 ± 0.06
	OPLS[e]	geom.	1.56 ± 0.11	2.06 ± 0.11	4.07 ± 0.15	2.51 ± 0.09
		arit.	1.53 ± 0.14	2.14 ± 0.17	3.94 ± 0.2	2.51 ± 0.12
Na^+	Jensen[f]	geom.	1.33 ± 0.15	2.03 ± 0.20	3.61 ± 0.26	2.41 ± 0.15
		arit.	1.24 ± 0.15	1.86 ± 0.21	3.36 ± 0.27	2.21 ± 0.15
K^+	CHARMM[b]	geom.	1.42 ± 0.15	2.24 ± 0.19	4.40 ± 0.28	2.49 ± 0.13
	GROMOS[d]	geom.	1.02 ± 0.24	1.59 ± 0.35	2.92 ± 0.45	1.96 ± 0.26
	OPLS[e]	geom.	0.99 ± 0.24	1.61 ± 0.47	2.93 ± 0.45	1.97 ± 0.25
	AMBER[e]	geom.	1.13 ± 0.18	1.73 ± 0.29	3.26 ± 0.45	2.08 ± 0.21
	Jensen[f]	geom.	0.89 ± 0.30	1.38 ± 0.44	2.61 ± 0.55	1.82 ± 0.32

[a] Ref 60. [b] Ref 62. [c] Ref 63. [d] Ref 61. [e] Ref 65. [f] Ref 64.

simulation of DPPC bilayers with potassium chloride[41] reveals that aggregation had begun, although not in the form of a large single cluster as reported here. Although it is obvious that the existence of aggregates limits the amount of free K^+ ions that may interact with the lipid oxygens, our results still suggest that the difference between small or negligible binding does not necessarily come from such artifacts. Finally, it is clear that the presence of these aggregates in the vicinity of the lipid bilayer does not affect the bilayer.

Structural Effects. There is ample discussion in the literature about how binding of different ions affects the ordering of the acyl chains as well as the orientation of the lipid head dipole in simulations. This includes alkaline and alkaline−earth ones.[26,40−42,44] Therefore, the present analysis will focus on differences due to force field parameters for the same ion. Lipid ordering may be monitored in different ways, but it is most easily observed as a decrease in area per lipid. The average values from the different simulations are shown in Table II. The simulation without ions exhibits an area per lipid of 0.620 nm^2, close to the experimental value of 0.64 nm^2. For the systems containing 0.2 M MCl (M represents K^+ or Na^+), the area is in some cases considerably smaller, in agreement with the previously reported results.[41] In the simulations containing Na^+ ions, the area per lipid varies from 0.531 to 0.593 nm^2, while those with K^+ ions show areas from 0.579 nm^2 up to the value in the salt-free system. In summary, the present simulations show that the binding of ions may reduce the area per lipid up to 15%. The data in Table II also shows a strong correlation between the decrease in area per lipid and the number of bound ions, which is clearly illustrated when these variables are plotted against each other in Figure 3.

The charge distribution in the PC head group can be represented by a dipole moment that is mainly due to the negatively charged phosphate group and the positively charged choline group. The contribution from each of the carbonyl groups is about 1 order of magnitude smaller. The orientation of the head group is sensitive to the local electrostatic field generated by neighboring atoms. Therefore,

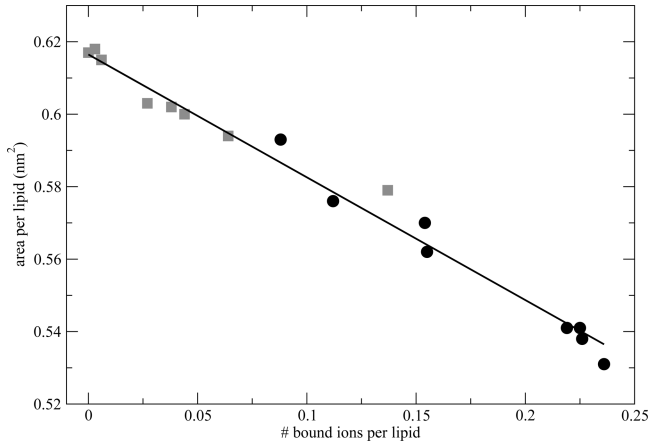

Figure 3. Area per lipid versus number of K^+ (gray squares) or Na^+ (black spheres) ions bound to the lipid bilayer. The line is a linear regression to both types of ions.

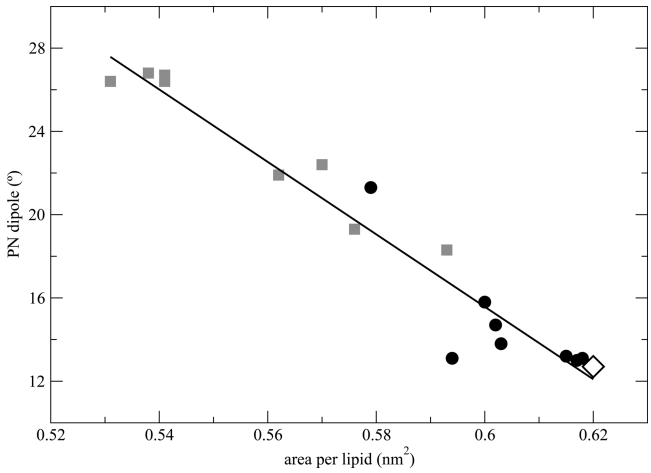

Figure 4. The **P**−**N** dipole tilt out of the membrane plane versus area per lipid. Data are displayed for Na^+ as black spheres and K^+ as gray squares. The line is a linear regression to both ions types. The unfilled diamond indicates the system without salt.

the orientation of the head group dipole is sensitive to the presence of ions[26,37,38,41] and acts as a charge sensor.[22,23] Here, the orientation of the dipole is measured as the (time and system) averaged angle between the **P**−**N** vectors and the bilayer plane. The results displayed in Table II show that whereas the system without ions exhibits an average angle of 13°, the binding of ions results in an increase of this value by 7−13°. Interestingly, the changes in the **P**−**N** tilt and the area per lipid are correlated as shown in Figure 4. This effect has already been observed when comparing simulations performed using different cutoff methods.[76] The reason for this correlation appears to be the balance between electrostatic energy and lipid packing. Thus, in the absence of ions, the **P**−**N** dipole tends to lie down close to the membrane plane reducing the electrostatic energy of the system. When ions are present, they screen the electrostatic interactions between the head groups and diminish the need of having the dipole close to the membrane plane. The tilt out of the membrane plane favors a closer lipid packing and reduces the area per lipid. In a similar way Grutovenko[39] correlated the presence of a chloride ion close a bilayer (within 1 nm

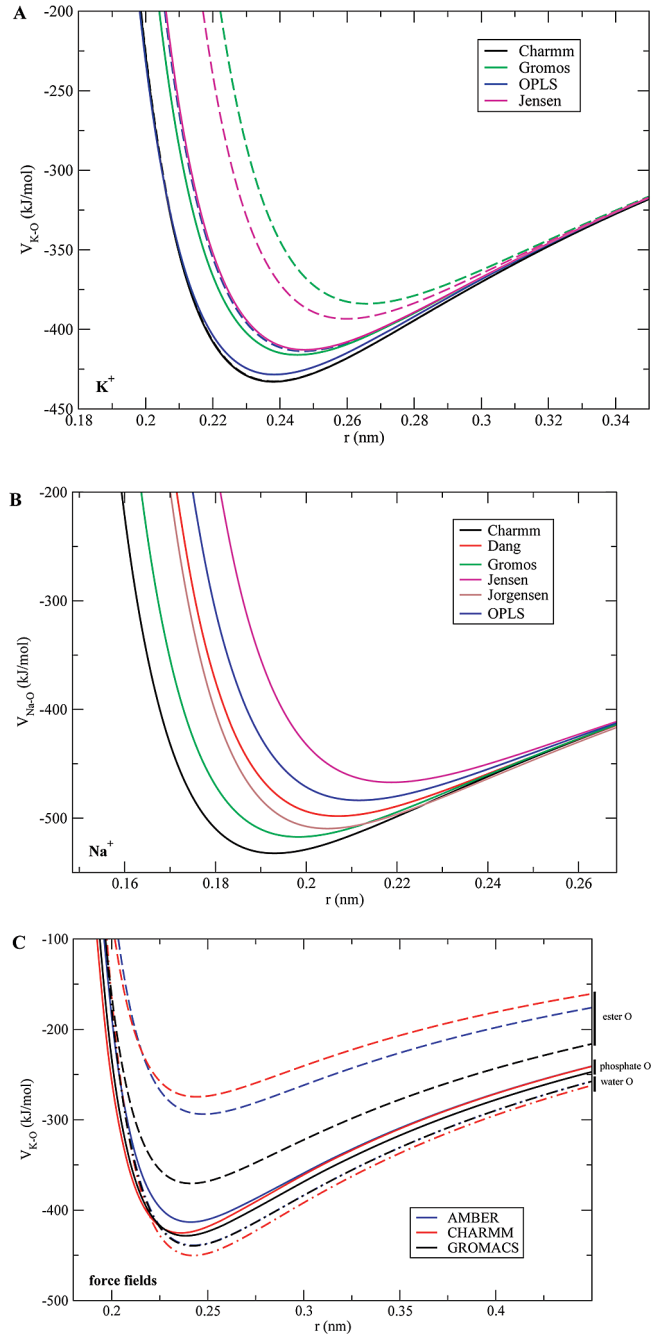

Figure 5. Cation−water/lipid oxygen potential energy function (Coulomb + LJ terms) for: (A) K^+−lipid phosphate oxygen pairs, (B) Na^+−lipid phosphate oxygen pairs, and (C) various K^+−water/lipid oxygen functions in different force fields (AMBER, CHARMM, and GROMOS, see Table IV). Full lines represent geometric and dashed lines arithmetic combination rules for σ. Results in B are only shown using geometric averages of σ's since the arithmetic averages produce results that are very similar (see Table II). Combination rules for σ are arithmetic in AMBER and CHARMM force fields and geometric for Berger's. Oxygen parameters are shown in Table IV. Corresponding AMBER, CHARMM, and OPLS K^+ parameters are displayed in Table I.

of a choline) with an increased dipole tilt of 12° out of the membrane plane.

The σ_{MO} Parameter. We also observe that the change in area per lipid and orientation of the lipid head group varies

Table IV. Fractional Charges and LJ Parameters for Lipid Phosphate, Lipid Ester, and Water Oxygens in Three Common Lipid Force Fields

Force field	atom	parameter	charge (*e*)	σ (nm)	ε (kJ/mol)
AMBER/GAFF	phosphate O	o	−0.780	0.2960	0.8786
	ester O	o	−0.570	0.2960	0.8786
	water O	ow (TIP3P)	−0.834	0.3151	0.6368
CHARMM	phosphate O	O2L	−0.780	0.3029	0.5021
	ester O	OBL	−0.520	0.3029	0.5021
	water O	OW (SPC)	−0.848	0.3166	0.6502
BERGER/OPLS	phosphate O	LO2	−0.800	0.2960	0.8780
	ester O	LO2	−0.700[a]	0.2960	0.8780
	water O	opls_111 (TIP3P)	−0.834	0.3151	0.6368

[a] This charge is −0.6 in one of the two chains (closer to those in the remaining force fields compared).

in a similar way as the ion hydration energies between the force fields (see Methods Section). Therefore, the degree of ion binding to the lipid bilayer is related to the energy of hydration that results from the parameters used, for which an estimate is given in Table II using the Born formula (see Methods Section). The average hydration energies are −425 ± 24 kJ/mol for Na^+ and −329 ± 17 kJ/mol for K^+, relatively close to the values of −382 and −302 kJ/mol obtained from experiments[77] and in good agreement with recent extensive simulations.[78] The main difference between the force fields studied here is the cation−oxygen potential energy function. In order to illustrate this difference, the K^+−O and Na^+−O interaction energy functions are shown in Figure 5A and B for different metal ion parameters but the same oxygen parameters (those of the phosphate oxygens of the lipid model used here). The position of the K^+−O minimum varies from 0.23 to 0.36 nm. In some cases, there are also substantial differences depending on whether the LJ radius was calculated as a geometric or arithmetic average. For the Na^+ ions, the differences are much smaller but still lead to distinctly different locations of the minima ranging from 0.19 to 0.22 nm. In the same way as in Figures 5A and B, we show in Figure 5C the K^+ −water/lipid oxygen potential energy functions for different types of oxygens in a few widely used force fields (see Table IV). It should be noted that the energy and location of the minima are similar for the different functions involving water oxygens and also lipid phosphate oxygens for the different water models and the K^+ parameters. The reasons for this are that the oxygen charge is similar in these cases (about −0.8), the cation parameters are transferable between SPC and TIP3P[65] water models and also the parameters compared provide similar Born energies. On the contrary, the function involving ester oxygens differs much more, mainly since the ester oxygen charges differ between the force fields (see Table IV). The larger carbonyl dipole in the Berger force field could explain the difference in preference of cations for phosphate or carbonyl lipid oxygens between simulations performed with this and other lipid force fields.[43]

The electrostatic attraction dominates the cation−oxygen interaction at long distances, while LJ repulsion dominates at short distances. The attractive part of the LJ interaction is, thus, always much smaller and, in most cases, negligible compared to the electrostatic contribution to the potassium−oxygen interaction. Since the electrostatic part is the same in all cases, it is the strength of the repulsive part of the LJ potential that controls the distance between the cation and the oxygen and the strength of binding. This is controlled by A_{MO} or σ_{MO} parameters, depending on which form of the LJ equation is used (see Table II and Methods Section).

Figure 6A shows the number of ions bound to the lipid oxygens versus σ_{MO} in the different simulations. There is a linear correlation between these two variables for σ_{MO} below 0.382 nm, while ion binding is weak or nonexistent for larger values. Similarly, Figures 4B and C show that both the area per lipid and the orientation of the lipid head group exhibit a similar linear correlation with σ_{MO} below 0.382 nm. The use of $A_{MO}^{1/12}$ instead of σ_{MO} as an independent variable gives similar linear correlations (not shown). The main result can be summarized as there is a threshold for σ_{MO} (or $A_{MO}^{1/12}$) above which ion binding is negligible. Above this value, the change in area per lipid or lipid head group dipole angle is, therefore, negligible. Below the threshold ion binding, areas per lipid as well as head group dipole tilt change linearly with the distance from the threshold.

Conclusions

The present work constitutes a systematic study of the effect of sodium and potassium LJ parameters on the ion binding to DPPC bilayers. For this purpose, a set of 200 ns simulations of DPPC bilayers in contact with 0.2 M aqueous salt solutions using different cation LJ parameters were performed. Eight trajectories with sodium chloride, nine with potassium chloride, and one without salt were generated.

The K^+ ions bind less to PC bilayers than Na^+ ions due to their larger radius. There are, however, large differences in binding of both ions depending on LJ parameters. For 0.2 M NaCl, different parameters give between 0.09 and 0.24 bound Na^+ ions per lipid, while the number of bound K^+ ions per lipid varies between 0 and 0.14 at the same concentration. The reason for the difference is that a larger ion has difficulties entering the head group region of the lipid bilayer. The size of the ions is determined by the balance between repulsive and attractive forces.

If these are just LJ ones, the σ_{MO} LJ parameter (where M is the cation and O is an oxygen) would be a good measure of the size. The LJ attraction between oppositely charged atoms is, however, negligible compared to that

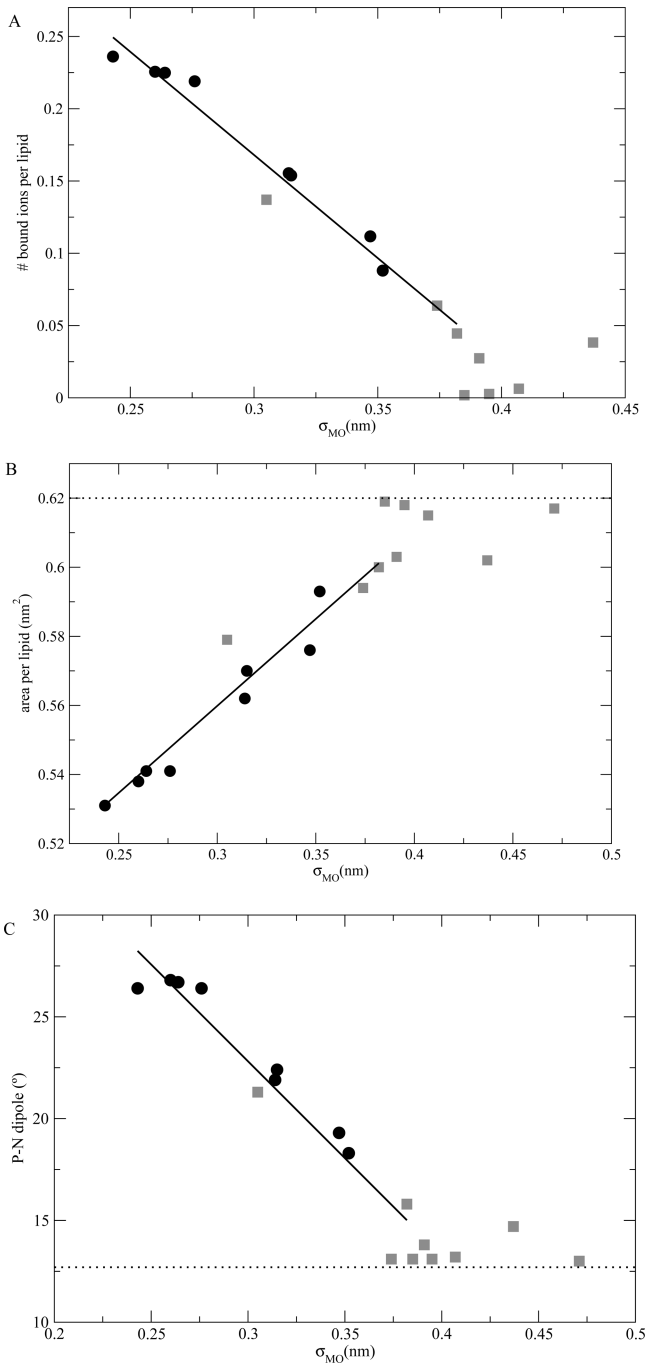

Figure 6. (A) Number of bound ions per lipid, (B) area per lipid, and (C) lipid head group (**P**−**N**) dipole tilt angle out the membrane plane versus the σ_{MO} parameters. The results are displayed for Na^+ as black spheres and K^+ as gray squares. The full lines are linear regressions excluding the simulations with $\sigma_{MO} > 0.382$ nm. The dotted lines in B and C indicate the area and the dipole tilt in the system without salt.

of the electrostatic attraction. Thus, one might argue that it would be more proper to use a measure for the radius that only includes the repulsive LJ parameter *A*. This parameter can, however, be expressed as $4\varepsilon\sigma$.[41] The electrostatic radius is, thus, proportional to $\sigma\varepsilon$ and only very weakly dependent upon the other van der Waals parameter, ε. This explains why only small differences are seen depending on which of the measures are used for the radius. The number of bound ions decreases with increasing radius, with a good linear correlation up to a maximum value of $\sigma_{MO} = 0.382$ nm above which binding disappears. This is reflected in area per lipid and helix dipole tilt, which covary with the amount of bound ions. The present results agree with our previous hypothesis that monovalent ions larger than K^+ (Rb^+ and Cs^+) do not bind to PC bilayers,[41] since their σ_{MO} are even larger than that of K^+.

Despite the differences observed with different force field parameters, the lack of accurate enough experimental results prohibits discerning the best parameters to be used in this type of simulation. However, the present results should be useful for selecting or calibrating new parameters when additional experimental information becomes available. It is clear that in systems were ions interact with large electrostatic dipoles or oppositely charged atoms, the attraction is dominated by electrostatics. The van der Waals attraction will then only play a negligible role and only the repulsive LJ (*A*) can be accurately determined from data for such systems. To determine the attractive parameter, *B*, one would need data for systems in which these LJ attraction interactions dominate, or at least are comparable to, electrostatic attraction. Such systems are rare, but this means also that the *B* parameter is of much less interest than the repulsive *A* parameter for ions. In any case, the present simulations show that the GROMOS and Åquist K^+ parameters should not be used with the Lorentz−Bertholet combination rule (arithmetic averaging of the σ's), since this produces unrealistic potassium chloride aggregation as an artifact. Both parameters were designed to be used with the other (geometrical) combination rule. Moreover, a new set of alkali and halide ion parameters became available for AMBER to overcome such aggregation problems[53] during the preparation of this manuscript. The new σ for K^+ has then been reduced and would give results closer to remaining sets tested here. This constitutes a warning not to mix parameters that are not self-consistent without careful tests. It is straightforward to extend the calibration scheme proposed here for Na^+ and K^+ to other ions, as long as the interactions can be properly modeled by classical pairwise electrostatic and LJ terms. Finally, the trends presented here using the TIP3P water model should also be valid for the other three site water models with minor quantitative differences, keeping in mind the slight differences between these models.

It is still uncertain if MD simulations to some extent exaggerate[43] the ion binding to lipid bilayers compared to the few experimental results reported thus far.[28,29] When comparing simulations, the degree of K^+ binding (if any) is still an open question. We do, here, reproduce the trend of previous studies in the sense that the larger the alkali ion, the less it binds to the membrane.[9,16,24,25,37,41] Moreover, present results reconcile previous MD studies of the binding of ions to PC bilayers.[41−43,54,56] However, there are other issues that need to be clarified, including other force field weaknesses and sampling artifacts.

Acknowledgment. The Spanish Ministry of Science and Technology supported this work through grant number SAF2008-04943-C02-01.

References

(1) Berkowitz, M. L.; Bostick, D. L.; Pandit, S. *Chem. Rev.* **2006**, *106*, 1527.

(2) Parsegian, V. A. *Ann. N.Y. Acad. Sci.* **1975**, *264*, 161.

(3) Elmore, D. E. *FEBS Lett.* **2006**, *580*, 144.

(4) Zhao, W.; Rog, T.; Gurtovenko, A. A.; Vattulainen, I.; Karttunen, M. *Biophys. J.* **2007**, *92*, 1114.

(5) Pandit, S. A.; Berkowitz, M. L. *Biophys. J.* **2002**, *82*, 1818.

(6) Mukhopadhyay, P.; Monticelli, L.; Tieleman, D. P. *Biophys. J.* **2004**, *86*, 1601.

(7) Pedersen, U. R.; Leidy, C.; Westh, P.; Peters, G. H. *Biochim. Biophys. Acta* **2006**, *1758*, 573.

(8) Loosley-Millman, M. E.; Rand, R. P.; Parsegian, V. A. *Biophys. J.* **1982**, *40*, 221.

(9) Tatulian, S. A. *Eur. J. Biochem.* **1987**, *170*, 413.

(10) Cunningham, B. A.; Gelerinter, E.; Lis, L. J. *Chem. Phys. Lipids* **1988**, *46*, 205.

(11) Altenbach, C.; Seelig, J. *Biochemistry* **1984**, *23*, 3913.

(12) Lis, L. J.; Lis, W. T.; Parsegian, V. A.; Rand, R. P. *Biochemistry* **1981**, *20*, 1771.

(13) Lis, L. J.; Parsegian, V. A.; Rand, R. P. *Biochemistry* **1981**, *20*, 1761.

(14) Herbette, L.; Napolitano, C. A.; McDaniel, R. V. *Biophys. J.* **1984**, *46*, 677.

(15) Akutsu, H.; Seelig, J. *Biochemistry* **1981**, *20*, 7366.

(16) Fukuma, T.; Higgins, M. J.; Jarvis, S. P. *Phys. Rev. Lett.* **2007**, *98*, 106101.

(17) Watts, A.; Harlos, K.; Marsh, D. *Biochim. Biophys. Acta* **1981**, *645*, 91.

(18) Hauser, H.; Shipley, G. G. *Biochemistry* **1984**, *23*, 34.

(19) Roux, M.; Bloom, M. *Biochemistry* **1990**, *29*, 7077.

(20) Clarke, R. J.; Lupfert, C. *Biophys. J.* **1999**, *76*, 2614.

(21) Brown, M. F.; Seelig, J. *Nature* **1977**, *269*, 721.

(22) Akutsu, H.; Nagamori, T. *Biochemistry* **1991**, *30*, 4510.

(23) Seelig, J.; Macdonald, P. M.; Scherer, P. G. *Biochem.* **1987**, *26*, 7535.

(24) Chapman, D.; Peel, W. E.; Kingston, B.; Lilley, T. H. *Biochim. Biophys. Acta* **1977**, *464*, 260.

(25) Binder, H.; Zschornig, O. *Chem. Phys. Lipids* **2002**, *115*, 39.

(26) Böckmann, R. A.; Hac, A.; Heimburg, T.; Grubmüller, H. *Biophys. J.* **2003**, *85*, 1647.

(27) Garcia-Manyes, S.; Oncins, G.; Sanz, F. *Biophys. J.* **2005**, *89*, 1812.

(28) Pabst, G.; Hodzic, A.; Strancar, J.; Danner, S.; Rappolt, M.; Laggner, P. *Biophys. J.* **2007**, *93*, 2688.

(29) Petrache, H. I.; Tristram-Nagle, S.; Harries, D.; Kucerka, N.; Nagle, J. F.; Parsegian, V. A. *J. Lipid Res.* **2006**, *47*, 302.

(30) van der Ploeg, P.; Berendsen, H. J. C. *J. Chem. Phys.* **1982**, *76*, 3271.

(31) Berger, O.; Edholm, O.; Jähnig, F. *Biophys. J.* **1997**, *72*, 2002.

(32) Feller, S. E. *Curr. Opin. Struct. Biol.* **2000**, *5*, 217.

(33) Tieleman, D. P.; Marrink, S. J.; Berendsen, H. J. C. *Biochim. Biophys. Acta* **1997**, *1331*, 235.

(34) Smondyrev, A. M.; Berkowitz, M. L. *J. Comput. Chem.* **1999**, *20*, 531.

(35) Lindahl, E.; Edholm, O. *Biophys. J.* **2000**, *79*, 426.

(36) Feller, S. E.; Gawrisch, K.; MacKerell, A. D., Jr. *J. Am. Chem. Soc.* **2002**, *124*, 318.

(37) Pandit, S. A.; Bostick, D.; Berkowitz, M. L. *Biophys. J.* **2003**, *84*, 3743.

(38) Sachs, J. N.; Nanda, H.; Petrache, H. I.; Woolf, T. B. *Biophys. J.* **2004**, *86*, 3772.

(39) Gurtovenko, A. A. *J. Chem. Phys.* **2005**, *122*, 244902.

(40) Böckmann, R. A.; Grubmüller, H. *Angew. Chem., Int. Ed.* **2004**, *43*, 1021.

(41) Cordomí, A.; Edholm, O.; Perez, J. J. *J. Phys. Chem. B* **2008**, *112*, 1397.

(42) Gurtovenko, A. A.; Vattulainen, I. *J. Phys. Chem. B* **2008**, *112*, 1953.

(43) Lee, S. J.; Song, Y.; Baker, N. A. *Biophys. J.* **2008**, *94*, 3565.

(44) Siu, S. W.; Vacha, R.; Jungwirth, P.; Bockmann, R. A. *J. Chem. Phys.* **2008**, *128*, 125103.

(45) Mark, P.; Nilsson, L. *J. Comput. Chem.* **2002**, *23*, 1211.

(46) Wallqvist, A.; Mountain, R. D. *Rev. Comput. Chem.* **1999**, *13*, 183.

(47) Guillot, B. *J. Mol. Liq.* **2002**, *101*, 219.

(48) Jorgensen, W. L.; Tirado-Rives, J. *Proc. Natl. Acad. Sci. U.S.A.* **2005**, *102*, 6665.

(49) Patra, M.; Karttunen, M. *J. Comput. Chem.* **2004**, *25*, 678.

(50) Auffinger, P.; Cheatham, T. E.; Vaiana, A. C. *J. Chem. Theory Comput.* **2007**, *3*, 1851.

(51) Chen, A. A.; Pappu, R. V. *J. Phys. Chem. B* **2007**, *111*, 11884.

(52) Chen, A. A.; Pappu, R. V. *J. Phys. Chem. B* **2007**, *111*, 6469.

(53) Joung, I. S.; Cheatham, T. E. *J. Phys. Chem. B* **2008**, *112*, 9020.

(54) Gurtovenko, A. A.; Vattulainen, I. *Biophys. J.* **2007**, *92*, 1878.

(55) Gurtovenko, A. A.; Vattulainen, I. *J Phys Chem B* **2008**, *112*, 1953.

(56) Lee, S. J.; Song, Y.; Baker, N. A. *Biophys. J.* **2008**, *94*, 3565.

(57) Lennard-Jones, J. E. *Proc. Phys. Soc., London* **1931**, *43*, 461.

(58) Berendsen, H. J. C.; van der Spoel, D.; van Drunen, R. *Comput. Phys. Commun.* **1995**, *91*, 43.

(59) Lindahl, E.; Hess, B.; van der Spoel, D. *J. Mol. Model.* **2001**, *7*, 306.

(60) Chandrasekhar, J.; Spellmeyer, D. C.; Jorgensen, W. L. *J. Am. Chem. Soc.* **1984**, *106*, 903.

(61) Straatsma, T. P.; Berendsen, H. J. C. *J. Chem. Phys.* **1988**, *89*, 5876.

(62) Beglov, D.; Roux, B. *J. Chem. Phys.* **1994**, *100*, 9050.

(63) Dang, L. X.; Kollman, P. A. *J. Phys. Chem.* **1995**, *99*, 55.

(64) Jensen, K. P.; Jorgensen, W. L. *J. Chem. Theory Comput.* **2006**, *2*, 1499.

(65) Åqvist, J. *J. Phys. Chem.* **1994**, *98*, 8253.

(66) Jorgensen, W. L.; Maxwell, D. S.; TiradoRives, J. *J. Am. Chem. Soc.* **1996**, *118*, 11225.

(67) Jorgensen, W. L.; Chandrasekhar, J.; Madura, J. D.; Impey, R. W.; Klein, M. L. *J. Chem. Phys.* **1983**, *79*, 926.

(68) Åqvist, J. *J. Phys. Chem.* **1990**, *94*, 8021.

(69) Babu, C. S.; Lim, C. *Chem. Phys. Lett.* **1999**, *310*, 225.

(70) Tunell, I.; Lim, C. *Inorg. Chem.* **2006**, *45*, 4811.

(71) Degreve, L.; Borin, A. C.; Mazze, F. M.; Rodrigues, A. L. G. *Chem. Phys.* **2001**, *265*, 193.

(72) Stephen, H.; Stephen, T.; *Solubilities of Inorganic and Organic Compounds*; Pergamon Press: Oxford, U.K., 1963.

(73) Vieira, D. S.; Degreve, L. *J. Mol. Struct. - THEOCHEM* **2002**, *580*, 127.

(74) Mazur, A. K. *J. Am. Chem. Soc.* **2003**, *125*, 7849.

(75) Cheatham, T. E. *Curr. Opin. Struct. Biol.* **2004**, *14*, 360.

(76) Wohlert, J.; Edholm, O. *Biophys. J.* **2004**, *87*, 2433.

(77) Marcus, Y. *Ion Properties;* Dekker: New York 1997.

(78) Kastenholz, M. A.; Hunenberger, P. H. *J. Chem. Phys.* **2006**, *124*.

CT9000763